

This article was downloaded by:[Us Naval Academy]
On: 13 September 2007
Access Details: [subscription number 770001558]
Publisher: Taylor & Francis
Informa Ltd Registered in England and Wales Registered Number: 1072954
Registered office: Mortimer House, 37-41 Mortimer Street, London W1T 3JH, UK



Biofouling

The Journal of Bioadhesion and Biofilm Research

Publication details, including instructions for authors and subscription information:
<http://www.informaworld.com/smpp/title~content=t713454511>

Effects of coating roughness and biofouling on ship resistance and powering

Michael P. Schultz ^a

^a Department of Naval Architecture and Ocean Engineering, United States Naval Academy, Annapolis, Maryland, USA

Online Publication Date: 01 October 2007

To cite this Article: Schultz, Michael P. (2007) 'Effects of coating roughness and biofouling on ship resistance and powering', *Biofouling*, 23:5, 331 - 341

To link to this article: DOI: 10.1080/08927010701461974

URL: <http://dx.doi.org/10.1080/08927010701461974>

PLEASE SCROLL DOWN FOR ARTICLE

Full terms and conditions of use: <http://www.informaworld.com/terms-and-conditions-of-access.pdf>

This article maybe used for research, teaching and private study purposes. Any substantial or systematic reproduction, re-distribution, re-selling, loan or sub-licensing, systematic supply or distribution in any form to anyone is expressly forbidden.

The publisher does not give any warranty express or implied or make any representation that the contents will be complete or accurate or up to date. The accuracy of any instructions, formulae and drug doses should be independently verified with primary sources. The publisher shall not be liable for any loss, actions, claims, proceedings, demand or costs or damages whatsoever or howsoever caused arising directly or indirectly in connection with or arising out of the use of this material.

Effects of coating roughness and biofouling on ship resistance and powering

MICHAEL P. SCHULTZ

Department of Naval Architecture and Ocean Engineering, United States Naval Academy, Annapolis, Maryland, USA

(Received 21 March 2007; accepted 15 May 2007)

Abstract

Predictions of full-scale ship resistance and powering are made for antifouling coating systems with a range of roughness and fouling conditions. The estimates are based on results from laboratory-scale drag measurements and boundary layer similarity law analysis. In the present work, predictions are made for a mid-sized naval surface combatant at cruising speed and near maximum speed. The results indicate that slime films can lead to significant increases in resistance and powering, and heavy calcareous fouling results in powering penalties up to 86% at cruising speed. The present estimates show good agreement with results from full-scale ship power trials.

Keywords: *Drag, powering, resistance, biofouling, roughness, antifouling coatings*

Introduction

The primary role of a ship antifouling (AF) coating system is to limit the increase in frictional drag as a result of surface deterioration and biofouling accumulation. Failure in this pursuit results in either increased power to maintain a given speed or reduced speed at a given input power, both of which have associated economic penalties (Townsin, 2003). The effect of coating condition is crucial to the performance of ships. Frictional drag alone can account for as much as 90% of the total drag on some hull types, even when the hull is relatively smooth and unfouled (Kempf, 1937). For this reason, a significant body of work has focused on better understanding the effect of coating roughness on frictional drag. A review of the early work in this field is given by Lackenby (1962). More recently, the research focused on assessing how changes in surface roughness affect the drag of the self-polishing copolymer (SPC) tributyl tin (TBT) systems (e.g. Musker, 1980–1981; Townsin et al. 1981; Granville, 1987; Medhurst, 1989; Grigson, 1992), with less effort given to quantifying the effect of fouling. This was likely due to the fact that the TBT systems provided long-term fouling control with minimal settlement of fouling organisms (e.g. Jelic-Mrcelic et al. 2006). However, these systems are facing a

worldwide ban in 2008 (Champ, 2003), and their primary replacement, copper-based paints, are not as effective in controlling fouling (Abbott et al. 2000). This has spurred active research for effective, non-toxic alternatives (e.g. Swain & Schultz, 1996; Carman et al. 2006; Genzer & Efimenko, 2006; Statz et al. 2006).

The impact of fouling on drag has long been noted, and much of the early work is reviewed by Anon (1952). Subsequent hydrodynamic research has included laboratory studies of the effects of biofilms (e.g. Watanabe et al. 1969; Picologlou et al. 1980; Schultz & Swain, 1999), filamentous algae (e.g. Kouwen & Unny, 1973; Schultz, 2000), and calcareous macrofouling (e.g. Leer-Andersen & Larsson, 2003; Schultz, 2004). Full-scale ship testing to document the effect of fouling on the drag of copper-based coatings has also been conducted (e.g. Lewthwaite et al. 1985; Haslbeck & Bohlander, 1992). The results of all these studies indicate that fouling leads to a significant increase in frictional drag, although the magnitude of the increase depends on the fouling type and coverage. It should be noted that despite the large body of research focused on understanding the impact of fouling on ship resistance, one issue which has yet to be satisfactorily addressed is how to define fouling coverage quantitatively so as to allow simple predictions of resistance and powering.

In the present paper, predictions of full-scale ship resistance and powering are made for a mid-sized naval surface combatant coated with AF systems with a range of roughness and fouling conditions operating at cruising speed and near maximum speed. The predictions are based on results from laboratory-scale drag measurements and boundary layer similarity law analysis. While the roughness and fouling conditions considered in this work are only representative (not exhaustive) and the predictions are for a single hull form, the methodology implemented here can be used for other fouling conditions and ship hull forms for which laboratory drag data are available. Future work is planned in which the economic impact of hull roughness and fouling is quantified for a range of ship types and operational scenarios using the methodology described herein.

Materials and methods

In this section, ship resistance and powering predictions based on scale model testing are discussed. Next, some basic characteristics of turbulent boundary layer flows and the impact of surface roughness on these flows are discussed. Finally, a method of relating laboratory measurements and observations to the full-scale frictional drag of a ship using boundary layer similarity laws is presented. (For nomenclature, see Appendix).

Prediction of ship resistance and powering using scale model tests

Estimates of ship resistance and power requirements are typically made through towing tank tests of a ship model that is geometrically similar to the full-scale ship. The total resistance (drag) of the ship model, R_{Tm} , is made up of two primary components. These are the residuary resistance, R_{Rm} , and the frictional resistance, R_{Fm} , as shown in Equation 1 (Gillmer & Johnson, 1982).

$$R_{Tm} = R_{Rm} + R_{Fm} \quad (1)$$

The residuary resistance is mainly due to wavemaking, while the frictional resistance is due to tangential shear stresses on the ship hull arising from the viscosity of the fluid. It is customary to express Equation 1 in its non-dimensional form. This is done by dividing by the reference dynamic pressure, $\frac{1}{2}\rho_m U_m^2$, and the wetted area of the ship model hull, S_m , where ρ_m is the fluid density for the model tests and U_m is the ship model towing speed. The total resistance coefficient of the model, C_{Tm} , is, therefore, the sum of the residuary resistance coefficient of the model, C_{Rm} , and the frictional resistance coefficient, C_{Fm} . The residuary resistance coefficient of the

model is a function of the Froude number, $Fr_m = U_m(gL_m)^{-1/2}$, where g is the acceleration due to gravity and L_m is the length of the model. Likewise, the frictional resistance coefficient of the model is a function of the Reynolds number, $Re_m = U_m L_m \nu_m^{-1}$, where ν_m is the kinematic viscosity of the fluid for the model tests. The total resistance coefficient of the model is, therefore, given as (Gillmer & Johnson, 1982)¹:

$$C_{Tm} = C_{Rm}(Fr_m) + C_{Fm}(Re_m) \quad (2)$$

In order to accurately predict the resistance of the full-scale ship with model tests, it is desirable to have dynamic similarity between the ship and the model. Equation 2 illustrates that in order to accomplish this, both the Froude number and the Reynolds number would have to be matched between the model and the ship. In practice, this is impossible to do. Instead incomplete dynamic similarity is used in which the Froude number of the model and the ship are matched as shown in Equation 3:

$$\begin{aligned} Fr_m &= Fr_s \\ \frac{U_m}{\sqrt{gL_m}} &= \frac{U_s}{\sqrt{gL_s}} \end{aligned} \quad (3)$$

where, U_s is the ship speed and L_s is the ship length. Towing tank tests are carried out at a range of model speeds corresponding to full-scale ship speeds in accordance with Equation 3, as shown below:

$$U_m = U_s \sqrt{\frac{L_m}{L_s}} = \frac{U_s}{\sqrt{\lambda}} \quad (4)$$

where, the scale ratio, $\lambda = L_s/L_m$. The total resistance coefficient, C_{Tm} , is measured at each speed. The frictional resistance coefficient, C_{Fm} , is obtained using the ITTC-1957 formula (Woo et al. 1983) given as:

$$C_{Fm} = \frac{0.075}{(\log_{10} Re_m - 2)^2} \quad (5)$$

The residuary resistance coefficient of the model, C_{Rm} , is then found using Equation 2. Since the residuary resistance is a function of the Froude number and $Fr_m = Fr_s$ in the model tests, it is understood that $C_{Rm} = C_{Rs}$. The frictional resistance coefficient of the ship, C_{Fs} , is also found using Equation 5 by substituting Re_s for Re_m . The total resistance coefficient of the ship, C_{Ts} , is given by Equation 6 (Gillmer & Johnson, 1982):

$$C_{Ts} = C_{Rs} + C_{Fs} + C_A \quad (6)$$

where, C_A is the correlation allowance. The correlation allowance is used to account for differences in

actual ship resistance typically due to scale effect on propeller characteristics, scale effect on the ship wake, the effect of three-dimensionality on the viscous resistance, and hull roughness (Woo et al. 1983). In the present work, the effect of hull roughness will be dealt with separately and will be accounted for in an added frictional resistance term, ΔC_{F_s} so the total resistance coefficient of the ship, C_{T_s} , is:

$$C_{T_s} = C_{R_s} + C_{F_s} + C_A + \Delta C_{F_s} \quad (7)$$

Figure 1 illustrates the relative contribution of resistance components for a typical naval ship over a range of Froude numbers. At low to moderate speeds ($Fr_s < 0.25$), the frictional resistance is the largest component of the total drag. At higher speeds, the residuary resistance becomes dominant. The results shown in Figure 1 are for a hydraulically smooth hull ($\Delta C_{F_s} = 0$). It should also be noted that the condition of the hull (i.e. coating roughness and fouling) has a direct influence on the frictional resistance, while having a negligible effect on the residuary resistance. An increase in hull roughness through coating condition or fouling would cause an increase in the frictional resistance leading to higher total drag. And, because of the aforementioned relative importance of the drag components, an increase in hull roughness would generally be expected to exert a greater influence at low to moderate speeds than at high speed.

The ship powering requirement in terms of shaft power, SP , is related to the total resistance and ship speed by Equation 8:

$$SP = \frac{R_{T_s} U_S}{PC} \quad (8)$$

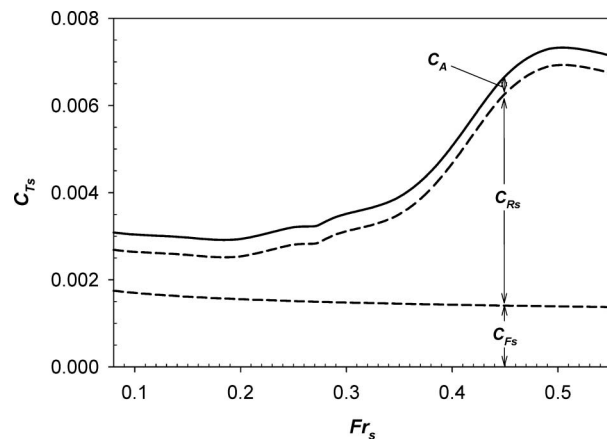


Figure 1. Graph of the total resistance coefficient, C_{T_s} , of a typical naval ship vs. Froude number, Fr_s . The dashed lines show the relative contribution of the resistance components. The correlation allowance, C_A is taken to be 0.0004 as suggested by Gillmer and Johnson (1982). The hull is assumed to be hydraulically smooth (i.e. $\Delta C_{F_s} = 0$).

where, PC = propulsive coefficient which represents the overall efficiency of the propeller and shafting.

Turbulent boundary layer background

In order to better understand the influence of coating roughness and fouling on ship resistance and powering, some basic characteristics of the mean velocity profile in a turbulent boundary layer and the effect of surface roughness will be discussed here. For more thorough coverage, the reader is asked to refer to Schlichting (1979) or Schultz and Swain (2000).

A boundary layer forms in the region of fluid adjacent to a ship's hull when it is underway. In this region, the motion of the fluid is impeded by its viscosity. At the hull (or wall), there is no relative motion between the fluid and the wall. This is called the no-slip condition. At some distance away from the wall, the mean velocity reaches its freestream value. A velocity gradient is generated due to these two boundary conditions. The region in which this velocity gradient exists is called the boundary layer. The boundary layer grows in thickness as one travels down the length of the hull.

The mean flow in a turbulent boundary layer is generally considered to consist of two layers, the inner and outer layer, each with its own scaling law. In the inner layer, the mean velocity, U , at a given distance from the wall, y , is determined by the friction velocity, U_τ , the kinematic viscosity, ν , and the roughness height, k . This is called the 'law of the wall' and is given by Schubauer and Tchen (1961):

$$\frac{U}{U_\tau} = f\left(\frac{yU_\tau}{\nu}, \frac{kU_\tau}{\nu}\right) \quad (9)$$

$$U^+ = f(y^+, k^+).$$

For the outer layer, von Kármán (1930) showed that the difference between the velocity at the outer edge of the boundary layer, U_e , and the local mean velocity, U , at a distance y from the wall is determined by the boundary layer thickness, δ and U_τ . This is called the 'velocity-defect law', given as:

$$\frac{U_e - U}{U_\tau} = g\left(\frac{y}{\delta}\right) \quad (10)$$

$$U_e^+ - U^+ = g\left(\frac{y}{\delta}\right).$$

If the inner and outer velocity profiles are matched (Equations 9 and 10), a logarithmic velocity profile results in the overlap region of the two layers ($\delta \gg y \gg \nu/U_\tau$). This is called the 'log-law' and was proposed by Millikan (1938) for smooth walls. For flows over smooth or rough walls, it can be expressed as:

$$U^+ = \frac{1}{\kappa} \ln(y^+) + B - \Delta U^+(k^+) \quad (11)$$

where, κ = von Kármán constant = 0.41, B = smooth-wall log-law intercept = 5.0, and ΔU^+ = roughness function (note that, for smooth walls, $\Delta U^+ \equiv 0$). The effect of surface roughness, therefore, is to cause a downward shift (ΔU^+) in the log-law velocity profile. This is indicative of an increased momentum deficit due to the roughness and is directly related to the increase in frictional drag of the surface.

The effect of increasing roughness Reynolds number, k^+ , on the mean velocity profile can be seen in the recent results of Schultz and Flack (2007) which were obtained in a zero pressure gradient, turbulent boundary layer using laser Doppler velocimetry on a rough surface consisting of diagonal scratches. The roughness height, k , is here taken to be the equivalent sand roughness height, k_s . This is the height of uniform, closely-packed sand which gives the same roughness function as the roughness of interest in the fully rough flow regime (Schlichting, 1979). The Figure shows that for small roughness Reynolds numbers ($k_s^+ < \sim 3$), the flow is unaffected by the roughness and $\Delta U^+ = 0$. This condition is called the hydraulically smooth regime. In this regime, the roughness elements are small enough so that any perturbations caused by them are completely damped out by viscosity. As the roughness Reynolds number increases, the roughness elements begin to produce pressure drag leading to an increase in the roughness function and frictional drag. This is called the transitionally rough flow regime. As the roughness Reynolds number continues to increase, at some point, the roughness is large enough so that the drag on the wall is entirely

due to the pressure drag on the roughness elements. This is called the fully rough flow regime.

The roughness function results corresponding to the mean velocity profiles shown in Figure 2 are presented in Figure 3. Also shown are the results of Shockling et al. (2006) for a similar roughness taken in a fully developed pipe flow. The Figure shows that the flow over this type of roughness is hydraulically smooth ($\Delta U^+ = 0$) for $k_s^+ \leq 3$ and by the time $k_s^+ \geq 25$, the flow is fully rough with the roughness function exhibiting a logarithmic dependence on k_s^+ . The limits of the hydraulically smooth and fully rough flow regimes depend, at least to some degree, on the roughness type. For example, Schlichting (1979) suggests limits of $k_s^+ \leq 5$ for hydraulically smooth flow and $k_s^+ \geq 70$ for fully rough flow over uniform, closely packed sand.

The outer region of a turbulent boundary layer is generally thought to be independent of surface roughness except for the role that the roughness plays in setting the velocity (U_τ) and length (δ) scales. Therefore, the velocity-defect law (Equation 10) is usually considered to be universal for both rough and smooth surfaces. The mean velocity profiles of Schultz and Flack (2007) are presented using outer scaling in Figure 4. Also included in the figure is a smooth wall profile ($k_s^+ \approx 0$). Excellent collapse of the mean velocity profiles is observed regardless of the roughness Reynolds number, thus supporting the concept of a universal velocity-defect law. Although the results shown in Figure 4 are for a single roughness type and height, Connelly et al. (2006) also recently demonstrated that a universal velocity-defect law applies for a range of roughness types and heights.

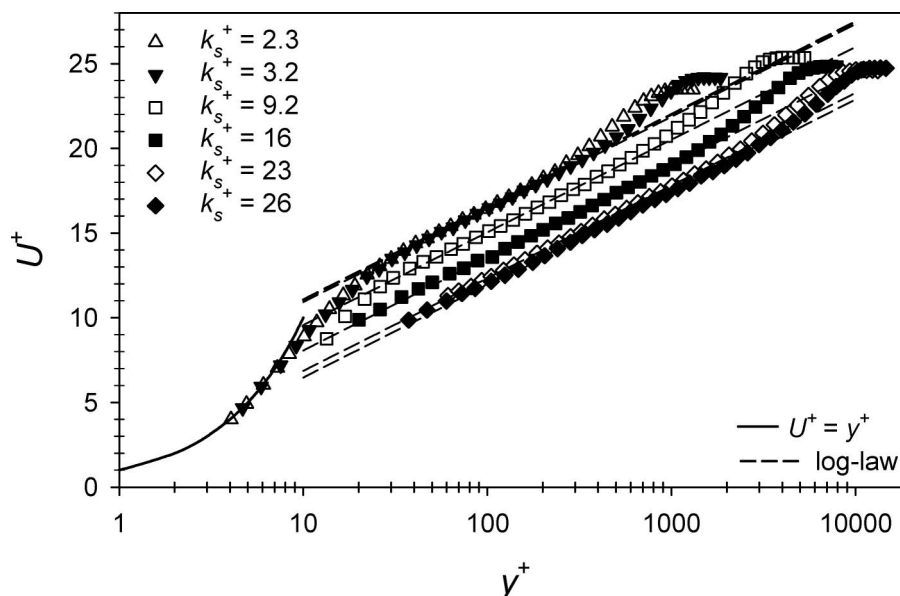


Figure 2. Graph of turbulent boundary layer, mean velocity profiles using inner (law of the wall) scaling. The profiles are from Schultz and Flack (2007) and illustrate the effect of increasing roughness Reynolds number, k_s^+ , on the law of the wall velocity profile.

Prediction of the change in frictional resistance at ship scale

The similarity between smooth and rough wall boundary layers which was shown in the previous section was utilised by Granville (1958, 1987) to develop a similarity law scaling procedure. This procedure allows one to predict the impact of a given roughness on the frictional drag of a plate of arbitrary length based on laboratory-scale measurements of the frictional drag and roughness function of a plate

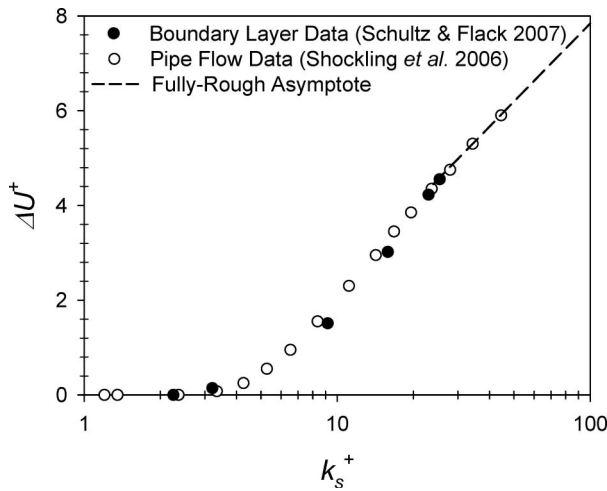


Figure 3. Graph of the roughness function, ΔU^+ , vs. roughness Reynolds number, k_s^+ . Data are from the boundary layer measurements of Schultz and Flack (2007) and fully developed pipe flow experiments of Shockling et al. (2006). The dashed line shows the asymptotic behaviour of the roughness function in the fully rough flow regime.

covered with the same roughness. In the present work, Granville’s similarity law scaling will be used to predict the change in frictional drag of a plate of ship length in order to model the change in frictional resistance of the ship itself (ΔC_{Fs}). This is a reasonable assumption since the effect of the pressure gradient resulting from the three dimensionality of the actual ship hull is embodied in the correlation allowance, and the pressure drag of the hull form itself is not expected to be altered dramatically by the roughness.

Granville’s similarity law scaling procedure is illustrated graphically in Figure 5. The procedure consists of first plotting the frictional resistance coefficient of a smooth plate as a function of $\log(Re)$. The results of Schultz (2002) showed that smooth plate laboratory data agreed well with the Kármán-Schoenherr friction line (Schoenherr, 1932) given as:

$$\frac{0.242}{\sqrt{C_F}} = \log(Re C_F). \tag{12}$$

The frictional resistance coefficient for the rough plate laboratory measurement is then plotted on the graph of C_F versus $\log(Re)$. This point coincides with the intersection of two loci. The first is the smooth friction line (Equation 12) displaced by a distance of $\Delta U^+ \kappa [\ln(10)]^{-1}$ in the positive $\log(Re)$ direction. The second locus is line of constant $L_{plate}^+ = L_{plate} U_\tau v^{-1}$ which satisfies the following relationship:

$$Re = \frac{L_{plate}^+}{\sqrt{\frac{C_F}{2} \left(1 - \frac{1}{\kappa} \sqrt{\frac{C_F}{2}}\right)}}. \tag{13}$$

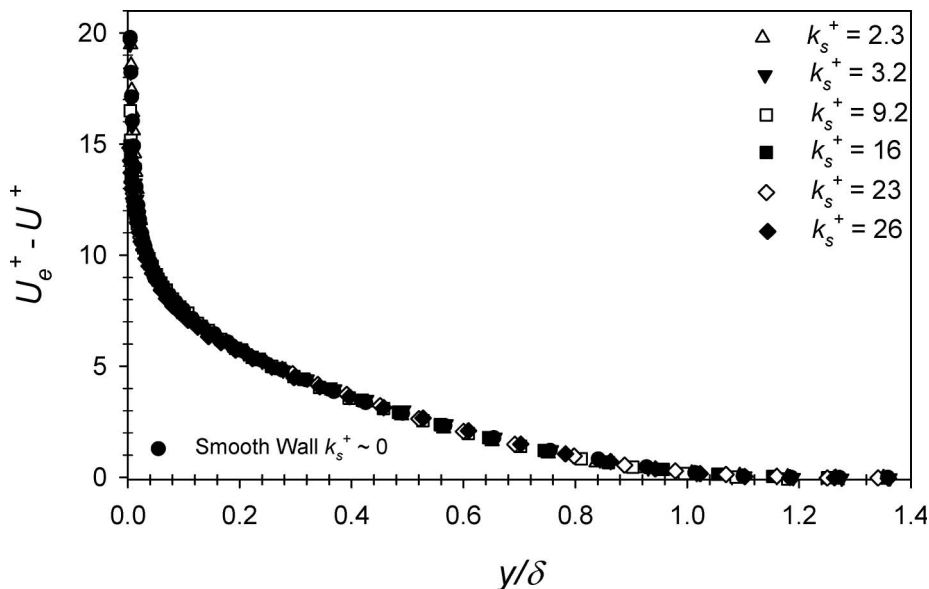


Figure 4. Graph of turbulent boundary layer, mean velocity profiles using outer (velocity-defect law) scaling. The profiles are from Schultz and Flack (2007) and illustrate the insensitivity of the outer layer to the surface roughness.

In order to determine C_{F_s} , the line of constant L_{plate}^+ is shifted a distance of $\log(L_s/L_{plate})$ in the positive $\log(Re)$ direction. The intersection of this line and the first locus identifies C_{F_s} . The increase in frictional resistance, ΔC_{F_s} , due to the roughness is the difference between C_{F_s} and the smooth value given by Equation 12 for a plate of length, L_s .

The present ship-scale frictional drag predictions are based on hydrodynamic measurements carried out at the US Naval Academy Hydromechanics Laboratory on 1.52 m long plates coated with AF coatings in the unfouled, fouled, and cleaned conditions. This work is detailed in Schultz (2004). In that study, both fouling-release and biocide-based AF systems were tested in the unfouled, fouled, and cleaned conditions. All the coatings tested exhibited an increase in frictional resistance in the unfouled

condition ranging from 3–7% compared to a hydraulically smooth surface. In the fouled condition, the increase in frictional resistance depended strongly on the fouling type with increases >100% for surfaces covered with calcareous fouling. When the surfaces were cleaned, the frictional drag returned to near, but slightly above, the unfouled condition due to coating deterioration and damage. From these measurements and further testing by the author over several more fouling and cleaning cycles, the hydrodynamic properties for a range of coating roughness and fouling conditions were generated in terms of k_s . These are shown in Table I.

The reader should note that these are representative conditions based on the measurements and observations given in Schultz (2004). They cannot, therefore, be expected to characterise all possible

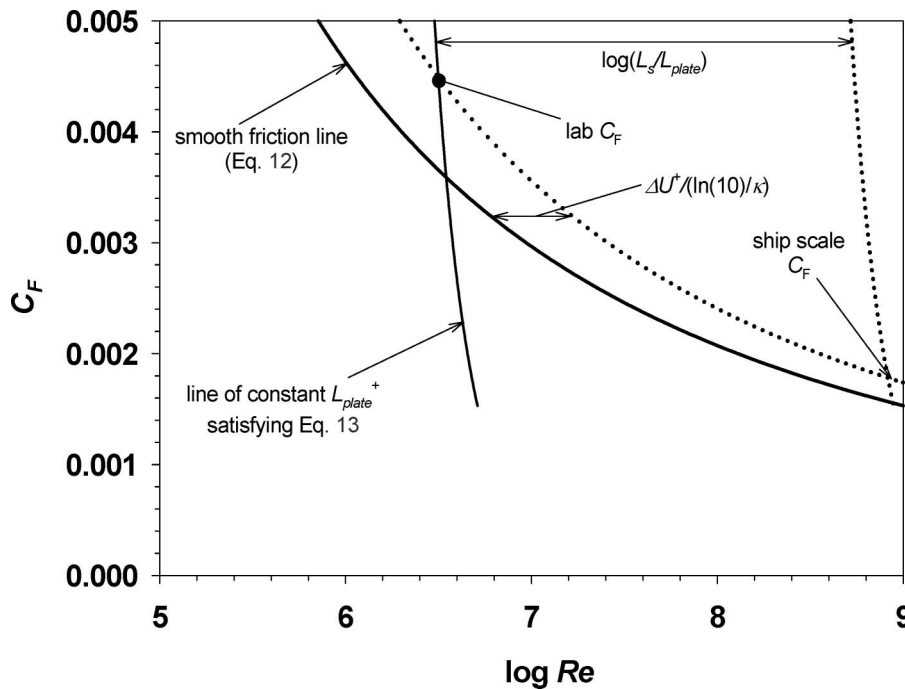


Figure 5. Graphical representation of Granville's similarity law scaling (Granville, 1958; 1987). The graph illustrates how the roughness function, ΔU^+ , determined from the laboratory hydrodynamic tests is related to the increase in the frictional resistance coefficient at ship scale, ΔC_{F_s} .

Table I. A range of representative coating and fouling conditions. The Naval Ships' Technical Manual (NSTM) rating is a fouling index used by the US Navy based on Naval Ships' Technical Manual (2002). The values of equivalent sand roughness height (k_s) and average coating roughness (Rt_{50}) are based on the measurements of Schultz (2004).

Description of condition	NSTM rating*	k_s (μm)	Rt_{50} (μm)
Hydraulically smooth surface	0	0	0
Typical as applied AF coating	0	30	150
Deteriorated coating or light slime	10–20	100	300
Heavy slime	30	300	600
Small calcareous fouling or weed	40–60	1000	1000
Medium calcareous fouling	70–80	3000	3000
Heavy calcareous fouling	90–100	10,000	10,000

*NSTM (2002).

coating or fouling conditions. For example, spatial heterogeneity in coating roughness and fouling and differences in fouling community composition all could have a significant effect on k_s and the resulting ΔC_{Fs} . Also shown in Table I are the estimated average hull roughness (Rt_{50}) for the different conditions and the US Navy fouling rating according to Naval Ships' Technical Manual (NSTM 2002). Rt_{50} is the maximum peak to trough roughness height measured over a sampling length of 50 mm which is a standard measure of coating roughness based on hull surveys using the BMT Hull Roughness Analyzer (Medhurst, 1990; Howell & Behrends, 2006). Rt_{50} is not generally used to characterise a fouled surface; therefore, the values given for these conditions in Table I represent the likely maximum peak to trough height of the fouling in each case. Chapter 081 of the NSTM (2002) is the document that the US Navy uses for guidance on underwater hull cleaning. The NSTM ratings shown in Table I are used by divers to evaluate the fouling condition of the hull *in situ*. Ratings of 30 or less are used to denote coverage of soft fouling only. A rating of 0 denotes a surface free of fouling, while a rating of 30 represents heavy coverage of soft fouling. A rating of 40 indicates a surface with incipient calcareous fouling. The rating increases with the severity of the calcareous fouling, with a rating of 100 denoting heavy coverage of large calcareous fouling of multiple types. Some distinction should also be drawn between light and heavy slime layers. Heavy slime would be a condition where the underlying paint colour is difficult or impossible to determine. In the light slime condition, the underlying paint colour is visible.

The paper of Woo et al. (1983) provides both full scale trial powering data as well as model drag and propeller results for the US Navy *Oliver Hazard Perry* class frigate (*FFG-7*). These data were used in the present work in order to assess the impact of coating roughness and fouling on the shaft power requirements (*SP*) of an *FFG-7* hull form. The *FFG-7* has a waterline length of 124.4 m with a beam of 14.3 m and displaces 3779 metric tonnes. The full-scale trials were carried out in seawater with $\rho = 1022.3 \text{ kg m}^{-3}$ and $\nu = 8.97 \times 10^{-7} \text{ m}^2 \text{ s}^{-1}$. The full-scale predictions herein were also made for these conditions. The ship was recently out of dry dock when the full-scale trials were conducted, and the average hull roughness (Rt_{50}) was estimated to be $150 \mu\text{m}$. The ship model tests were conducted on a 1:20.82 scale model at the Naval Surface Warfare Center, Carderock, MD, USA. Further details are given in Woo et al. (1983).

The data from the model tests were used to predict the full-scale shaft powering requirements of the *FFG-7* using the procedures previously outlined in this paper. The correlation allowance (C_A) was taken

to be 0.0004 as suggested by Gillmer and Johnson (1982) for a similar hull form. The change in the frictional resistance coefficient (ΔC_{Fs}) resulting from the hull roughness was calculated using similarity law scaling procedure (Granville, 1958; 1987) for $Rt_{50} = 150 \mu\text{m}$ ($k_s = 30 \mu\text{m}$). It was assumed for this calculation, as well as the subsequent ones presented in this paper, that the roughness function follows the results of Schultz and Flack (2007) and Shockling et al. (2006) shown in Figure 3. While it is known that the roughness function is not universal for all roughness types in the transitionally rough flow regime (Grigson, 1992), the results of Schultz (2004) agree reasonably well with this roughness function for a range of coating roughness and fouling conditions. The procedure for calculating ΔC_{Fs} is as follows: i) The value of k_s for a given hull condition is selected based on Table I; ii) an initial value of k_s^+ is assumed; iii) the corresponding roughness function (ΔU^+) is determined from Figure 3; iv) the viscous length scale (ν/U_τ) is determined as k_s/k_s^+ ; v) the value of L_{plate}^+ is determined as L_{plate} divided by the viscous length scale ($L_{plate} = 1.52 \text{ m}$ in the study of Schultz, 2004); vi) the two loci of Granville's procedure are located. (a) The first is a line of L_{plate}^+ from step v satisfying Equation 13; (b) the second is Equation 12 offset by $\Delta U^+ \kappa [\ln(10)]^{-1}$ in the positive $\log(Re)$ direction; vii) the ship scale frictional resistance coefficient (C_{Fs}) is located by the intersection of the second locus and the first locus shifted a distance of $\log(L_s/L_{plate})$ in the positive $\log(Re)$ direction; viii) the corresponding value of Re_s is obtained from the graph. If Re_s is the value desired, the procedure is complete. If it is too low, a larger k_s^+ is used and steps iii–viii are repeated. If Re_s is too high, a smaller k_s^+ is used and steps iii–viii are repeated; ix) the increase in frictional resistance, ΔC_{Fs} , due to the roughness is the difference between C_{Fs} and the smooth value given by Equation 12 for a plate of length, L_s ; x) ΔC_{Fs} is used in Equations 7 and 8 to predict the resulting *SP*.

Results and discussion

The predictions of the full-scale powering of the *FFG-7* from model test results were made for ship speeds of 7.7 m s^{-1} (15 knots) and 15.4 m s^{-1} (30 knots), which correspond to a typical cruising speed and nearly full speed, respectively. These predictions along with the results of the full-scale trials of Woo et al. (1983) are presented in Figure 6. The agreement between the predictions and the full-scale trials results is excellent (within 1.5% at both speeds).

Predictions of the change in total resistance were carried out for the same two ship speeds for all of the coating roughness and fouling conditions shown in Table I. These are shown in Table II for a ship speed

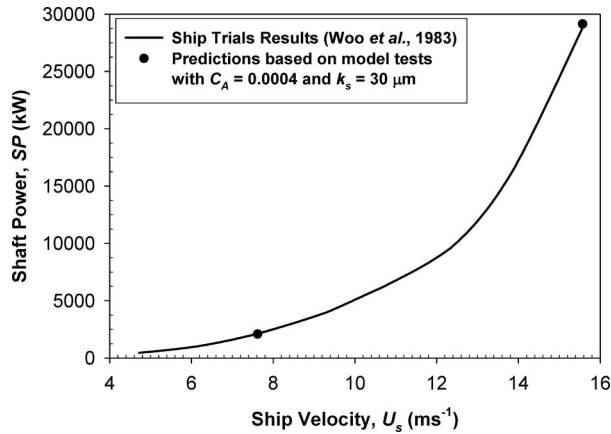


Figure 6. Graph of required shaft power (SP) vs ship speed (U_s) for an *FFG-7* frigate. The solid line shows the results of the full-scale trials of Woo et al. (1983). The filled circles are the predictions based on the present method using the model test data of Woo et al. (1983) with $C_A = 0.004$. The prediction used similarity law scaling for a typical as applied AF coating ($Rt_{50} = 150 \mu\text{m}$; $k_s = 30 \mu\text{m}$).

Table II. Predictions of the change in total resistance (ΔR_T) for an *Oliver Hazard Perry class* frigate (*FFG-7*) with a range of representative coating and fouling conditions at a speed of 7.7 m s^{-1} (15 knots).

Description of condition	$\Delta R_T @ U_s = 7.7 \text{ m s}^{-1}$ (kN)	% $\Delta R_T @ U_s = 7.7 \text{ m s}^{-1}$
Hydraulically smooth surface	–	–
Typical as applied AF coating	4.6	2%
Deteriorated coating or light slime	23	11%
Heavy slime	41	20%
Small calcareous fouling or weed	69	34%
Medium calcareous fouling	105	52%
Heavy calcareous fouling	162	80%

of 7.7 m s^{-1} (15 knots). The results indicate that only a small resistance penalty ($\sim 2\%$) is expected to result from a typical, as applied AF coating compared to a hydraulically smooth hull. With coating deterioration or a light slime layer, the impact on resistance begins to become significant ($\sim 11\%$ increase in R_T). The resistance penalty continues to increase with the severity of fouling until, for a heavy layer of calcareous fouling, the total resistance is nearly doubled at cruising speed ($\sim 89\%$ increase in R_T).

The predictions of the change in total resistance for a ship speed of 15.4 m s^{-1} (30 knots) are shown in Table III. The percentage increase in resistance due to hull roughness and fouling ranges from 4–55%.

Table III. Predictions of the change in total resistance (ΔR_T) for an *Oliver Hazard Perry class* frigate (*FFG-7*) with a range of representative coating and fouling conditions at a speed of 15.4 m s^{-1} (30 knots). Also presented is the percentage decrease in speed for a fixed shaft power.

Description of condition	$\Delta R_T @ U_s = 15.4 \text{ m s}^{-1}$ (kN)	% $\Delta R_T @ U_s = 15.4 \text{ m s}^{-1}$
Hydraulically smooth surface	–	–
Typical as applied AF coating	46	4%
Deteriorated coating or light slime	118	10%
Heavy slime	192	16%
Small calcareous fouling or weed	305	25%
Medium calcareous fouling	447	36%
Heavy calcareous fouling	677	55%

In general, the percentage increases at this speed are lower than at cruising speed. This is due to the smaller relative contribution of frictional resistance compared to the residuary resistance at high speed. The lone exception is the typical, as applied AF coating. This surface goes from operating nearly in the hydraulically smooth flow regime at cruise ($k_s^+ \sim 7$) to well into the transitionally rough flow regime at high speed ($k_s^+ \sim 14$). This explains the rise in total resistance penalty at high speed for this particular condition. It should be noted that the maximum equivalent sand roughness height (k_s) to maintain a hydraulically smooth surface does depend on the type of ship and its speed. For the *FFG-7*, the maximum value of k_s for hydraulically smooth conditions is $\sim 13.5 \mu\text{m}$ at 15 knots and is $\sim 7 \mu\text{m}$ at 30 knots. This value tends to increase with ship length, and it decreases with ship speed.

Predictions of the change in required shaft power were also carried out. These are shown in Table IV for a ship speed of 7.7 m s^{-1} (15 knots). The reader should note that the change in required shaft power presented here accounts not only for the increase in total hull resistance but also for the increased propeller loading at a given speed due to the hull fouling, which can lead to a significant reduction in the propulsive coefficient for the heavier fouling conditions. These changes in propulsive efficiency were calculated based on the open water propeller test results presented in Woo et al. (1983). The powering results again indicate that only a small penalty ($\sim 2\%$) is expected to result from a typical, as applied AF coating compared to a hydraulically smooth hull. With coating deterioration or a light slime layer, the impact on powering begins to become significant ($\sim 11\%$ increase in SP). The

powering penalty continues to increase with the severity of fouling until, for a heavy layer of calcareous fouling, the required power is increased by 86%.

The predictions of the change in required shaft power for a ship speed of 15.4 m s^{-1} (30 knots) are shown in Table V. The percentage powering penalty due to hull roughness and fouling ranges from 4–59%. In general, the percentage increases at this speed are lower than at cruising speed for the same reason as was discussed in the resistance results. Also presented in Table V is the percentage reduction in speed at a fixed input shaft power of $2.7 \times 10^4 \text{ kW}$, the required shaft power for the hydraulically smooth hull at 15.4 m s^{-1} (30 knots). The analysis shows that the percentage reduction in speed ranges from 0.9–10.7%. This corresponds to a speed loss of 0.14 m s^{-1} to 1.6 m s^{-1} (0.28–3.2 knots).

Although there are relatively few full-scale trial results in the literature for hull forms similar to the *FFG-7*, some comparisons between the ones that exist and the present predictions will be made.

Table IV. Predictions of the change in required shaft power (ΔSP) for an *Oliver Hazard Perry class* frigate (*FFG-7*) with a range of representative coating and fouling conditions at a speed of 7.7 m s^{-1} (15 knots).

Description of condition	$\Delta SP @ U_s = 7.7 \text{ m s}^{-1}$ (kW)	% $\Delta SP @ U_s = 7.7 \text{ m s}^{-1}$
Hydraulically smooth surface	–	–
Typical as applied AF coating	50	2%
Deteriorated coating or light slime	250	11%
Heavy slime	458	21%
Small calcareous fouling or weed	781	35%
Medium calcareous fouling	1200	54%
Heavy calcareous fouling	1908	86%

Hundley and Tate (1980) conducted a series of ship powering trials on *USS Harold E. Holt*, a *Knox class* frigate. When operating with a clean propeller and a hull fouled with ‘light grass’ and 10–20% coverage of ‘incipient tube worm growth’, the required shaft power (SP) at 7.7 m s^{-1} (15 knots) was 4525 kW. The SP after the hull was cleaned was 3650 kW. Therefore, the increase in required power that can be attributed to the fouling is 24%. The fouling condition from the present paper that best coincides with the pre-cleaning *Holt* power trial is the ‘small calcareous fouling or weed’ condition. In this condition, the SP is predicted to be 2989 kW at 7.7 m s^{-1} (15 knots). It is not as clear what the post-cleaning hull roughness was on the *Holt*, but it would be expected to have been between the ‘typical as applied AF coating’ and ‘deteriorated coating’ conditions. The predicted power requirements in these conditions are 2258 kW and 2457 kW, respectively. Therefore, a 22–32% increase in SP due to the fouling is predicted by present method, which is in good agreement with the measured increase of 24% on a similar hull form.

Haslbeck and Bohlander (1992) conducted full-scale sea trials in order to quantify the effect of slime layers on ship powering. In their study, power trials were conducted on the *USS Brewton*, another *Knox class* frigate. The ship was coated with an ablative AF paint containing both cuprous oxide and TBT and had been subject to fouling in Pearl Harbor, Hawaii for 22 months. An initial hull inspection indicated the presence of a fairly heavy slime film with little to no calcareous fouling. Power trials were conducted in which the shaft power and ship speed were measured. Subsequently, the ship was cleaned and power trials were performed again. After cleaning, the average hull roughness (Rt_{50}) was measured to be $264 \mu\text{m}$ using the BMT Hull Roughness Analyzer. A difference in required shaft power of 9% at a ship speed of 8.2 m s^{-1} (16 knots) was measured between the two power trials. This is most appropriately represented by the difference between the

Table V. Predictions of the change in required shaft power (ΔSP) for an *Oliver Hazard Perry class* frigate (*FFG-7*) with a range of representative coating and fouling conditions at a speed of 15.4 m s^{-1} (30 knots). Also presented is the percentage decrease in speed for a fixed shaft power.

Description of condition	$\Delta SP @ U_s = 15.4 \text{ m s}^{-1}$ (kW)	% $\Delta SP @ U_s = 15.4 \text{ m s}^{-1}$	% reduction in speed for fixed $SP = 2.7 \times 10^4 \text{ kW}$
Hydraulically smooth surface	–	–	–
Typical as applied AF coating	1004	4%	0.9%
Deteriorated coating or light slime	2618	10%	2.7%
Heavy slime	4311	16%	4.0%
Small calcareous fouling or weed	6934	26%	5.8%
Medium calcareous fouling	10,329	38%	7.5%
Heavy calcareous fouling	16,043	59%	10.7%

'heavy slime' and the 'deteriorated coating' conditions in the present work. At cruising speed (7.7 m s^{-1} or 15 knots), the predicted SP in the 'heavy slime' condition is 2666 kW. Given the aforementioned prediction for the 'deteriorated coating', the increase in required power resulting from the fouling is 8%. This is in very good agreement with the full-scale trials.

Full-scale trials documenting the effect of heavy calcareous fouling are presented in *Marine Fouling and Its Prevention* (Anon, 1952). Unfortunately, the hull forms reported on (two 1920–1930s era destroyers and a World War II era battleship) differ significantly from the present frigate. This makes direct comparisons impractical. However, at cruising speed an increase of 60–110% in required shaft power was measured for these hull forms. A reduction in maximum speed at a fixed input power of 9% was observed for destroyer with a maximum speed similar to the *FFG-7*. These results, therefore, are similar to the present predictions.

Conclusions

A method of predicting the impact of coating roughness and fouling on the frictional resistance and powering of a full-scale ship has been presented. The prediction relies on results from laboratory-scale ship model tests along with boundary layer similarity law scaling to assess the impact of the surface condition on the frictional resistance. The method was illustrated for an *Oliver Hazard Perry class* frigate (*FFG-7*). The results show that a typical, as applied AF coating suffers fairly small penalties in required shaft power at both cruising speed and near top speed. A deteriorated coating or light slime film is predicted to cause a significant increase in required shaft power for this hull form. Heavy calcareous fouling is predicted to increase required shaft power by 86% as compared to a hydraulically smooth hull at cruising speed. Comparisons of the present results with full-scale trials of similar hull forms reported in the literature show good agreement. Future plans are to utilise this methodology to assess the economic impact of hull roughness and fouling to the entire US Navy fleet. Another area for future work is to better address the role that spatial heterogeneity in coating roughness and fouling and differences in fouling community composition have on the resulting drag and powering penalties. In the present work, the roughness and fouling was assumed to have a homogeneous distribution over the entire hull. This is typically not the case, and significant variation is often observed. At present, it is not altogether clear the influence this will have. Hydrodynamic measurements on surfaces with significant heterogeneity in roughness and fouling may serve to further elucidate this.

Acknowledgements

The author gratefully acknowledges the financial support of this research by the Office of Naval Research. Thanks are also due to Mr Bill Beaver and Mr Zseleczky and to the referees for their many helpful comments and suggestions.

Note

1. An alternative approach to ship resistance and powering prediction from scale model tests is to assume that the total resistance is comprised of wavemaking and viscous components (International Towing Tank Conference [ITTC], 1978). This is generally referred to as the ITTC-78 method. In this method, the viscous component is assumed to be due to both frictional resistance and pressure or form resistance. The ITTC-78 procedure explicitly accounts for the form resistance as a form factor multiplied by the frictional resistance. In the present procedure employed by the US Navy (e.g. Gillmer & Johnson, 1982; Woo et al. 1983), the form resistance is implicitly accounted for in the residuary resistance, and no form factor is used. It should be noted that the resistance and powering predictions from the two methods are generally comparable.

References

- Abbott A, Abel PD, Arnold DW, Milne A. 2000. Cost-benefit analysis of the use of TBT: the case for a treatment approach. *Sci Total Environ* 258:5–19.
- Anon. 1952. *Marine fouling and its prevention*. Annapolis, MD: US Naval Institute.
- Carman ML, Estes TG, Feinberg AW, Schumacher JF, Wilkerson W, Wilson LH, Callow ME, Callow JA, Brennan AB. 2006. Engineered antifouling microtopographies – correlating wettability with cell attachment. *Biofouling* 22:11–21.
- Champ MA. 2003. Economic and environmental impacts on port and harbors from the convention to ban harmful marine anti-fouling systems. *Mar Pollut Bull* 46:935–940.
- Connelly JS, Schultz MP, Flack KA. 2006. Velocity-defect scaling for turbulent boundary layers with a range of relative roughness. *Exp Fluids* 40:188–195.
- Genzer J, Efimenko K. 2006. Recent developments in superhydrophobic surfaces and their relevance to marine fouling: a review. *Biofouling* 22:339–360.
- Gillmer TC, Johnson B. 1982. *Introduction to naval architecture*. Annapolis, MD: US Naval Institute.
- Granville PS. 1958. The frictional resistance and turbulent boundary layer of rough surfaces. *J Ship Res* 2:52–74.
- Granville PS. 1987. Three indirect methods for the drag characterization of arbitrarily rough surfaces on flat plates. *J Ship Res* 31:70–77.
- Grigson CWB. 1992. Drag losses of new ships caused by hull finish. *J Ship Res* 36:182–196.
- Haslbeck EG, Bohlender G. 1992. Microbial biofilm effects on drag – lab and field. *Proc SNAME Ship Production Symp*. Paper No. 3A-1. 7 p.
- Howell D, Behrends B. 2006. A review of surface roughness in antifouling coatings illustrating the importance of cutoff length. *Biofouling* 22:401–410.
- Hundley LL, Tate CW. 1980. Hull-fouling studies and ship powering trial results on seven FF 1052 class ships. DW Taylor Naval Ship Research & Development Center Report # DTNSRDC-80/027. 111 p.

- International Towing Tank Conference (ITTC) 1978. Proc 15th International Towing Tank Conference: report of performance committee. The Hague.
- Jelic-Mrcelic G, Sliskovic M, Antolic B. 2006. Biofouling communities on test panels coated with TBT and TBT-free copper-based antifouling paints. *Biofouling* 22:293–302.
- Kempf G. 1937. On the effect of roughness on the resistance of ships. *Trans INA* 79:109–119.
- Kouwen N, Unny TE. 1973. Flexible roughness in open channels. *ASCE J Hydraulics Division* 99:713–728.
- Lackenby H. 1962. Resistance of ships, with special reference to skin friction and hull surface condition. *Proc Inst Mechl Eng* 176:981–1014.
- Leer-Andersen M, Larsson L. 2003. An experimental/numerical approach for evaluating skin friction on full-scale ships with surface roughness. *J Mar Sci Technol* 8:26–36.
- Lewthwaite JC, Molland AF, Thomas KW. 1985. An investigation into the variation of ship skin frictional resistance with fouling. *Trans R Inst Naval Architects* 127:269–284.
- Millikan CM. 1938. A critical discussion of turbulent flows in channels and circular tubes. *Proc 5th Int Congr Appl Mechanics*, Cambridge, MA. pp 386–392.
- Medhurst JS. 1989. The systematic measurement and correlation of the frictional resistance and topography of ship hull coatings, with particular reference to ablative antifouling. PhD Thesis, University of Newcastle-upon-Tyne, UK.
- Medhurst JS. 1990. Outline of a draft international standard for the measurement and characterisation of roughness topography in fluid flow. London: Royal Institute of Naval Architects. March 1990. 9 p.
- Musker AJ. 1980–1981. Universal roughness functions for naturally-occurring surfaces. *Trans Can Soc Mech Eng* 1:1–6.
- Naval Ships' Technical Manual. 2002. Waterborne underwater hull cleaning of Navy ships. Publication # S9086-CQ-STM-010/CH-081R4. Naval Sea Systems Command. 31 p.
- Picologlou BF, Zelter N, Characklis WG. 1980. Biofilm growth and hydraulic performance. *ASCE J Hydraulics Div* 106:733–746.
- Schlichting H. 1979. Boundary-layer theory. 7th ed. New York: McGraw-Hill.
- Schoenherr KE. 1932. Resistances of flat surfaces moving through a fluid. *Trans SNAME* 40:279–313.
- Schubauer GB, Tchen CM. 1961. Turbulent flow. New Jersey, USA: Princeton University Press.
- Schultz MP. 2000. Turbulent boundary layers on surfaces covered with filamentous algae. *ASME J Fluids Eng* 122:357–363.
- Schultz MP. 2002. The relationship between frictional resistance and roughness for surfaces smoothed by sanding. *ASME J Fluids Eng* 124:492–499.
- Schultz MP. 2004. Frictional resistance of antifouling coating systems. *ASME J Fluids Eng* 126:1039–1047.
- Schultz MP, Swain GW. 1999. The effect of biofilms on turbulent boundary layers. *ASME J Fluids Eng* 121:733–746.
- Schultz MP, Swain GW. 2000. The influence of biofilms on skin friction drag. *Biofouling* 15:129–139.
- Schultz MP, Flack KA. 2007. The rough-wall turbulent boundary layer from the hydraulically smooth to the fully rough regime. *J Fluid Mech* 580:381–405.
- Shockling MA, Allen JJ, Smits AJ. 2006. Roughness effects in turbulent pipe flow. *J Fluid Mech* 564:267–285.
- Statz A, Finlay J, Dalsin J, Callow M, Callow JA, Messersmith PB. 2006. Algal antifouling and fouling-release properties of metal surfaces coated with a polymer inspired by marine mussels. *Biofouling* 22:391–399.
- Swain GW, Schultz MP. 1996. The testing and evaluation of non-toxic antifouling coatings. *Biofouling* 10:187–197.
- Townsin RL. 2003. The ship hull fouling penalty. *Biofouling* 19(Suppl.):9–16.
- Townsin RL, Byrne D, Svensen TE, Milne A. 1981. Estimating the technical and economic penalties of hull and propeller roughness. *Trans SNAME* 89:295–318.
- von Kármán T. 1930. Mechanische Ähnlichkeit und turbulenz. *Nachr Ges Wiss Göttingen* 58–76.
- Watanabe S, Nagamatsu N, Yokoo K, Kawakami Y. 1969. The augmentation in frictional resistance due to slime. *J Kansai Soc Naval Architects* 131:45–51.
- Woo EL, Karafiath G, Borda G. 1983. Ship-model correlation of powering performance on USS Oliver Hazard Perry, FFG-7 class. *Mar Technol* 20:35–52.

Appendix

C_A = correlation allowance

C_F = frictional resistance coefficient = $\frac{R_F}{\frac{1}{2}\rho U^2 S}$

C_R = residuary resistance coefficient = $\frac{R_R}{\frac{1}{2}\rho U^2 S}$

C_T = total resistance coefficient = $\frac{R_T}{\frac{1}{2}\rho U^2 S}$

ΔC_F = change in the frictional resistance coefficient due to hull roughness/fouling

Fr = Froude number = $\frac{U}{\sqrt{gL}}$

g = gravitational acceleration

k = roughness height

k_s = equivalent sand roughness height

k = roughness height

L = waterline length

L_{plate} = length of flat plate used in laboratory experiment

R_F = frictional resistance

R_R = residuary resistance

R_T = total resistance

ΔR_T = change in total resistance

Re = Reynolds number = $\frac{UL}{\nu}$

Rt_{50} = maximum peak to trough height over a 50 mm sampling length

PC = propulsive coefficient

S = wetted surface area of the hull

SP = shaft power = $\frac{R_T U}{PC}$

ΔSP = $SP_{rough} - SP_{smooth}$

U = velocity

U_e = velocity at outer edge of the boundary layer

U_τ = friction velocity = $\sqrt{\frac{\tau_w}{\rho}}$

ΔU^+ = roughness function

y = distance from the wall

δ = boundary layer thickness

λ = scale ratio = $\frac{L_s}{L_m}$

ν = fluid kinematic viscosity

ρ = fluid density

τ_w = wall shear stress

Superscript

+ = normalised by U_τ or v/U_τ

Subscripts

m = model

$rough$ = for actual surface condition

s = ship

$smooth$ = for hydraulically smooth surface condition